Article

The Palladium-Catalyzed Cross-Coupling Reaction of Carboxylic Anhydrides with Arylboronic Acids: A DFT Study

Lukas J. Goossen, Debasis Koley, Holger L. Hermann, and Walter Thiel

J. Am. Chem. Soc., **2005**, 127 (31), 11102-11114• DOI: 10.1021/ja052435y • Publication Date (Web): 16 July 2005

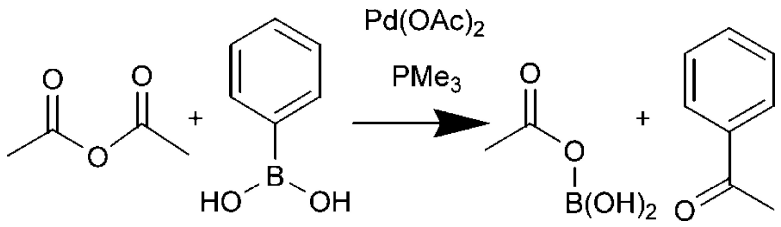

More About This Article

Additional resources and features associated with this article are available within the HTML version:

- Supporting Information
- Links to the 19 articles that cite this article, as of the time of this article download
- Access to high resolution figures
- Links to articles and content related to this article
- Copyright permission to reproduce figures and/or text from this article

View the Full Text HTML

J|A|C|S
ARTICLES
Published on Web 07/16/2005

The Palladium-Catalyzed Cross-Coupling Reaction of Carboxylic Anhydrides with Arylboronic Acids: A DFT Study

Lukas J. Goossen,*,‡ Debasis Koley, Holger L. Hermann, and Walter Thiel*

Contribution from the Max-Planck-Institut für Kohlenforschung, D-45470 Mülheim an der Ruhr, Germany

Received April 14, 2005; E-mail: goossen@chemie.uni-kl.de

Abstract: The mechanism of the cross-coupling of phenylboronic acid with acetic anhydride, a viable model of the widely used Suzuki reaction, has been studied by DFT calculations at the BP86/6-31G* level of theory. Two alternative catalytic cycles have been investigated, one starting from a neutral $Pd(0)L_2$ complex, the other from an anionic "Jutand-type" $[Pd(0)L_2X]^-$ species. The reaction profiles are in good agreement with the experimental findings, as both pathways require only moderate activation energies. Both pathways are dominated by cis-configured square-planar palladium(II)diphosphine intermediates. Despite careful investigations, we did not find in this model reaction any evidence for five-coordinate palladium(II) intermediates, which are commonly believed to cause the profound effects of counterions in palladium-catalyzed transformations. Instead, our calculations suggest that the higher catalytic activity of anionic complexes, such as $[Pd(PMe_3)_2OAc]^-$, may arise from their stronger ability to coordinate to carbon electrophiles. The transmetalation sequence is the same for both catalytic cycles, involving the dissociation of one phosphine ligand from the palladium. In the decisive transition state, in which the phenyl group is transferred from boron to palladium, the acetate base is found to be in a bridging coordination between these two atoms.

1. Introduction

Palladium-catalyzed cross-coupling reactions of arylboronic acids are powerful synthetic tools broadly applied throughout research laboratories and industrial production.[1] The most prominent example is the Suzuki coupling of aryl halides with arylboronic acids, which due to its high selectivity and the mild reaction conditions is the method of choice for the synthesis of biaryls (Scheme 1). In the last few decades, numerous related palladium-catalyzed couplings have been developed, for example, for the synthesis of dienes,[2] arylacetic acids,[3] or aryl ketones.[4]

Despite their enormous synthetic importance, the mechanism of such reactions is still not fully understood. The initially proposed catalytic cycle ("textbook mechanism") consists of an oxidative addition of the aryl halide to a coordinatively unsaturated $Pd(0)L_2$ species, followed by a transmetalation step in which the aryl residue is transferred from boron to palladium, and finally a reductive elimination to provide the biaryl product (Scheme 2).[1] Unfortunately, this mechanism provides no explanation for the pronounced influence exerted on catalytic activities by counterions, originating from either palladium(II) precatalysts or added metal salts.[5] One way to rationalize these effects is via the more complex reaction mechanism proposed by Amatore and Jutand, which involves an additional, faster catalytic cycle that starts from a three-coordinate anionic $[Pd(0)L_2X]^-$ species and involves five-coordinate palladium-(II) intermediates.[5] However, while the existence of anionic $[Pd(0)L_2X]^-$ species could meanwhile be confirmed both spectroscopically and by theoretical studies,[6,7] there still is no proof for the existence of five-coordinate intermediates.[6,8]

Scheme 1. Suzuki Biaryl Synthesis

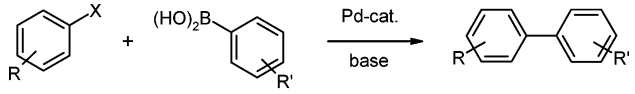

X = Br, Cl, I, N_2^+, OTf...

‡ Current address: Fachbereich Chemie - Organische Chemie, Technische Universität Kaiserslautern, Erwin-Schrödinger-Strasse, D-67663 Kaiserslautern, Germany. E-mail: goossen@chemie.uni-kl.de.

(1) (a) Miyaura, N.; Suzuki, A. *Chem. Rev.* **1995**, *95*, 2457. (b) Suzuki, A. *J. Organomet. Chem.* **1999**, *576*, 147. (c) Ishiyama, T.; Miyaura, N. *J. Organomet. Chem.* **2000**, *611*, 392. (d) Suzuki, A. in *Metal-Catalyzed Cross-Coupling Reactions*; Diederich, F., Stang, P. J., Eds.; Wiley-VCH: Weinheim, Germany 1998; p. 49.

(2) (a) Miyaura, N.; Yamada, K.; Suzuki, A. *Tetrahedron Lett.* **1979**, *20*, 3437. (b) Miyaura, N.; Yamada, K.; Suginome, H.; Suzuki, A. *J. Am. Chem. Soc.* **1985**, *107*, 972. (c) Miyaura, N.; Suzuki, A. *Org. Synth.* **1990**, *68*, 130. (d) Satoh, M.; Miyaura, N.; Suzuki, A. *Chem. Lett.* **1986**, 1329. (e) Miyaura, N.; Satoh, M.; Suzuki, A. *Tetrahedron Lett.* **1981**, *22*, 127.

(3) Goossen, L. J. *Chem. Commun.* **2001**, *7*, 669.

(4) (a) Goossen, L. J.; Ghosh, K. *Angew. Chem., Int. Ed.* **2001**, *40*, 3458. (b) Goossen, L. J.; Ghosh, K. *Eur. J. Org. Chem.* **2002**, *19*, 3254. (c) Goossen, L. J.; Winkel, L.; Döhring, A.; Ghosh, K.; Paetzold, J. *Synlett* **2002**, *8*, 1237. (d) Goossen, L. J.; Ghosh, K. *Chem. Commun.* **2001**, *20*, 2084. (e) Nagayama, K.; Shimizu, I.; Yamamoto, A. *Chem. Lett.* **1998**, 1143. (f) Kakino, R.; Kamusi, S.; Shimizu, I.; Yamamoto, A. *Bull. Chem. Soc. Jpn.* **2002**, *75*, 137.

(5) (a) Amatore, C.; Jutand, A. *Acc. Chem. Res.* **2000**, *33*, 314. (b) Amatore, C.; Azzabi, M.; Jutand, A. *J. Am. Chem. Soc.* **1991**, *113*, 1670. (c) Amatore, C.; Jutand, A.; Suarez, A. *J. Am. Chem. Soc.* **1993**, *115*, 9531. (d) Amatore, C.; Jutand, A.; M'Barki, M. A. *Organometallics* **1992**, *11*, 3009. (e) Amatore, C.; Carré, E.; Jutand, A.; M'Barki, M. A.; Meyer, G. *Organometallics* **1995**, *14*, 5605.

10.1021/ja052435y CCC: $30.25

Scheme 2. "Textbook" (outer cycle) and "Amatore−Jutand" (inner cycle) Mechanisms for Cross-Coupling Reactions

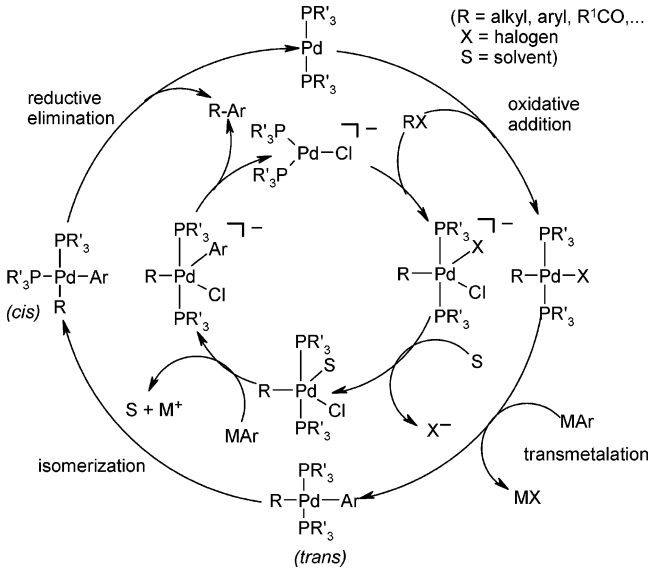

In-depth mechanistic studies as well as theoretical calculations on Suzuki coupling are difficult since the reaction mixtures tend to be extremely complex. In most protocols, the catalysts are generated in situ from palladium(II) salts and phosphine ligands, and the reaction mixtures contain not only arylboronic acids and aryl halides but also bases, coordinating solvents, and sometimes further additives.[1] Thus, a great variety of palladium species can potentially be formed, which all must be considered as possible intermediates in the catalytic process. This complexity, especially in the later stages of the reaction, is probably the main reason there are only very few mechanistic studies on the Suzuki coupling,[1a,9] in contrast to related reactions, such as hydroborations[10] or Heck olefinations.[5a,d,e,11]

In this article, we use density functional theory (DFT) to investigate the mechanism of palladium-catalyzed cross-coupling reactions. We have chosen to focus not on the classic Suzuki biaryl synthesis, but on the conceptually very similar cross-coupling of carboxylic anhydrides with boronic acids.[4] This aryl ketone synthesis, itself of high synthetic interest and versatility, is believed to proceed via an analogous mechanism (Scheme 2, R = COMe, X = OCOMe), and the similarity between the oxidative addition of aryl halides and anhydrides is already well-documented.[12,13]

Scheme 3. Cross-Coupling of Acetic Anhydride with Phenylboronic Acid

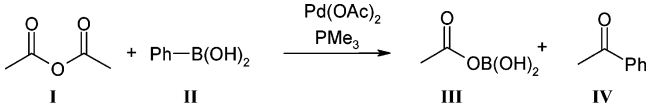

While this coupling reaction contains all important features of the Suzuki biaryl synthesis, it can be reduced to much greater simplicity without becoming unrealistic. The most elementary but still experimentally viable model system is the reaction of acetic anhydride with phenylboronic acid in the presence of a palladium(II)acetate/trimethylphosphine catalyst (Scheme 3). In this reaction, the acetate ion plays a triple role as the leaving group, the base, and the counterion in the palladium(II) precursor, so that the overall number of possible intermediates is greatly reduced.

Using density functional theory (BP86/6-31G*), we have computed two full catalytic cycles for this model reaction, one starting from a neutral $Pd(0)L_2$ complex, and the other one from the "Jutand-type" anionic $[Pd(0)L_2X]^-$ species (Scheme 4), which have been established as intermediates in Heck reactions.[5a,d,e,14] These are the first complete catalytic cycles that have been calculated for the coupling of carbon electrophiles with boronic acids, and to the best of our knowledge, they are also the first computational studies on transmetalation reactions of boronic acids in general. To minimize the computational effort, we have chosen the ligand to be trimethylphosphine ($L = PMe_3$), which is smaller and more electron-rich than the triarylphosphines that are commonly used in experimental studies.[12] In contrast to the corresponding triarylphosphine complexes, palladium(0) complexes of PMe_3 undergo facile oxidative addition reactions with anhydrides even at room temperature.[12] For this reason, the calculations for our model system are expected to yield a rather low barrier for the oxidative addition and a relatively high barrier for the reductive elimination compared with the systems investigated experimentally. However, once a viable reaction pathway for this model system has been identified, it can serve as the starting point for studies on more realistic systems with larger phosphine ligands.

The general features of the calculated cycles shown in Scheme 4 are consistent with the proposed mechanisms outlined in Scheme 2. However, there are also some striking differences. While the "textbook mechanism" mainly proceeds via trans-configured palladium(II)diphosphine complexes (Scheme 2), cis-configured intermediates dominate in the calculated catalytic cycles (Scheme 4). Moreover, according to the proposition of Amatore and Jutand, the anionic pathway involves five-coordinate species, whereas we find only four-coordinate intermediates, in qualitative agreement with related calculations on the oxidative addition of aryl halides to anionic palladium(0) complexes.[6,8] Interestingly, the transmetalation step is predicted to proceed via the same pathway for both catalytic cycles (Scheme 4).

(6) (a) Goossen, L. J.; Koley, D.; Hermann, H.; Thiel, W. *Chem. Commun.* **2004**, 2141. (b) Goossen, L. J.; Koley, D.; Hermann, H.; Thiel, W. *Organometallics* **2005**, *24*, 2398.
(7) (a) Kozuch, S.; Shaik, S.; Jutand, A.; Amatore, C. *Chem.—Eur. J.* **2004**, *10*, 3072. (b) Kozuch, S.; Amatore, C.; Jutand, A.; Shaik, S. *Organometallics* **2005**, *24*, 2319.
(8) Sundermann, A.; Uzan, O.; Martin, J. M. L. *Chem.—Eur. J.* **2001**, *7*, 1703.
(9) (a) Hills, I. D.; Netherton, M. R.; Fu, G. C. *Angew. Chem., Int. Ed.* **2003**, *42*, 5749. (b) Eberhardt, J. K.; Fröhlich, R.; Würthwein, E.-U. *J. Org. Chem.* **2003**, *68*, 6690.
(10) (a) Cui, Q.; Musaev, D. G.; Morokuma, K. *Organometallics* **1998**, *17*, 1383 and references therein. (b) Dorigo, A. E.; Schleyer, P. v. R. *Angew. Chem., Int. Ed. Engl.* **1995**, *34*, 115.
(11) (a) Albert, K.; Gisdakis, P.; Rösch, N. *Organometallics* **1998**, *17*, 1608. (b) Deeth, R. J.; Smith, A.; Brown, J. M. *J. Am. Chem. Soc.* **2004**, *126*, 7144. (c) Balcells, D.; Maseras, F.; Keay, B. A.; Ziegler, T. *Organometallics* **2004**, *23*, 2784. (d) Deeth, R. J.; Smith, A.; Hii, K. K.; Brown, J. M. *Tetrahedron Lett.* **1998**, *39*, 3229. (e) Hii, K. K.; Claridge, T. D. W.; Brown, J. M.; Smith, A.; Deeth, R. J. *Helv. Chim. Acta* **2001**, *84*, 3043. (f) von Schenck, H.; Akermark, B.; Svensson, M. *J. Am. Chem. Soc.* **2003**, *125*, 3503. (g) Ludwig, M.; Stromberg, S.; Svensson, M.; Akermark, B. *Organometallics* **1999**, *18*, 970.
(12) (a) Nagayama, K.; Kawataka, F.; Sakamoto, M.; Shimizu, I.; Yamamoto, A. *Chem. Lett.* **1995**, 367. (b) Kakino, R.; Narahashi, H.; Shimizu, I.; Yamamoto, A. *Bull. Chem. Soc. Jpn.* **2002**, *75*, 1333.
(13) Jutand, A.; Négri, S.; de Vries, J. G. *Eur. J. Inorg. Chem.* **2002**, 1711.
(14) Complexes involving palladium ligated to acetate ions have never been proposed by Amatore−Jutand in cross-coupling reactions. Nevertheless, $Pd(0)(PPh_3)_2(OAc)^-$ can be the active species in the oxidative addition in all reactions (including Suzuki reactions), as soon as acetate ions are present in a catalytic reaction as introduced by $Pd(OAc)_2$ or a base (Jutand, A. private communication, 2005).

Scheme 4. Main Intermediates of the Calculated Catalytic Cycles Starting from Either a Neutral or an Anionic Palladium Species

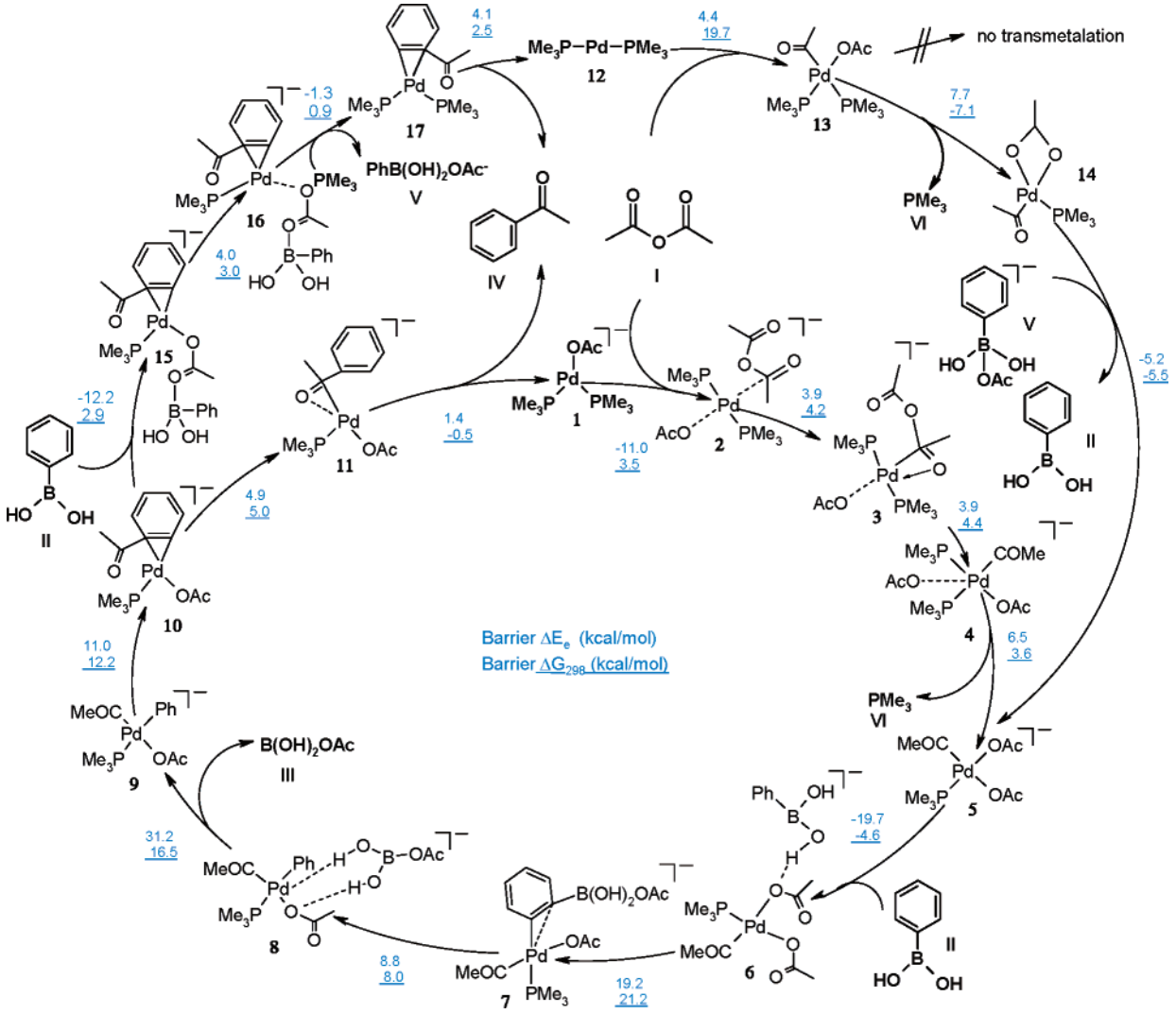

2. Computational Details

All calculations were performed with the Gaussian98 and Gaussian03 suites of programs.[15] The DFT calculations employed the BP86 functional[16,17] using the standard 6-31G* basis[18] for all atoms, except for palladium which was described by the LANL2DZ valence basis set in combination with the corresponding effective core potential.[19] Geometries were fully optimized, normally without symmetry constraints. Harmonic force constants were computed at the optimized geometries to characterize the stationary points as minima or saddle points. Zero-point vibrational corrections were determined from the harmonic vibrational frequencies to convert the total energies, E_e, to ground-state energies, E_0. The rigid-rotor harmonic-oscillator approximation was applied for evaluating the thermal and entropic contributions that are needed to derive the enthalpies, H_{298}, and Gibbs free enthalpies, G_{298}, at 298 K. Transition states were located from a linear transit scan in which the reaction coordinate was kept fixed at different distances, while all other degrees of freedom were optimized. After the linear transit search, the transition states were optimized using the default Berny algorithm implemented in the Gaussian code.[15] In critical cases, the nature of a given transition state was analyzed by IRC (Intrinsic Reaction Coordinate) computations.

For further validation, single-point BP86 calculations were performed at the optimized BP86/6-31G* geometries employing a larger basis set (EXT). Palladium was described by a Stuttgart−Dresden quasirelativistic pseudopotential and the associate (8s7p5d)/[6s5p3d] valence basis set;[20] the 6-31+G* basis was employed for B, C, O, and P, and the 6-31G** basis for all H atoms[18] (abbreviated as BP86/EXT). Single-point solvent calculations were performed at the optimized gas-phase geometries for all of the intermediates and transition states, using the CPCM[21] approach, which is an implementation of the conductor-like screening solvation model (COSMO)[22] in Gaussian03; THF was chosen as solvent (dielectric constant $\epsilon = 7.58$) with UAHF (United Atom Hartree−Fock) radii for the respective atoms (Pd, H, B, C, O, P). The charge distribution around the metal center was analyzed using Weinhold's NPA (Natural Population Analysis) approach.[23]

(15) Frisch, M. J. et al. *Gaussian 03*, revision B.05; Gaussian, Inc.: Pittsburgh, PA, 2003.
(16) Becke, A. D. *Phys. Rev. A* **1988**, *33*, 3098.
(17) Perdew, J. P. *Phys. Rev. B* **1986**, *33*, 8822.
(18) Hehre, W. J.; Radom, L.; Schleyer, P. v. R.; Pople, J. A. *Ab Initio Molecular Orbital Theory*; Wiley: New York, 1986.
(19) Hay, P. J.; Wadt, W. R. *J. Chem. Phys.* **1985**, *82*, 299.
(20) Andrae, D.; Häussermann, U.; Dolg, M.; Stoll, H.; Preuss, H. *Theor. Chim. Acta* **1990**, *77*, 123.
(21) (a) Barone, V.; Cossi, M. *J. Phys. Chem. A* **1998**, *102*, 1995. (b) Cossi, M.; Rega, N.; Scalmani, G.; Barone, V. *J. Comput. Chem.* **2003**, *24*, 669.
(22) (a) Klamt, A.; Schüürmann, G. *J. Chem. Soc., Perkin Trans. 2* **1993**, 799. (b) Schäfer, A.; Klamt, A.; Sattel, D.; Lohrenz, J. C. W.; Eckert, F. *Phys. Chem. Chem. Phys.* **2000**, *2*, 2187.
(23) (a) Reed, A. E.; Curtiss, L. A.; Weinhold, F. *Chem. Rev.* **1988**, *88*, 899. (b) Glendening, E. D.; Reed, A. E.; Carpenter, J. E.; Weinhold, F. *NBO*, version 3.1.

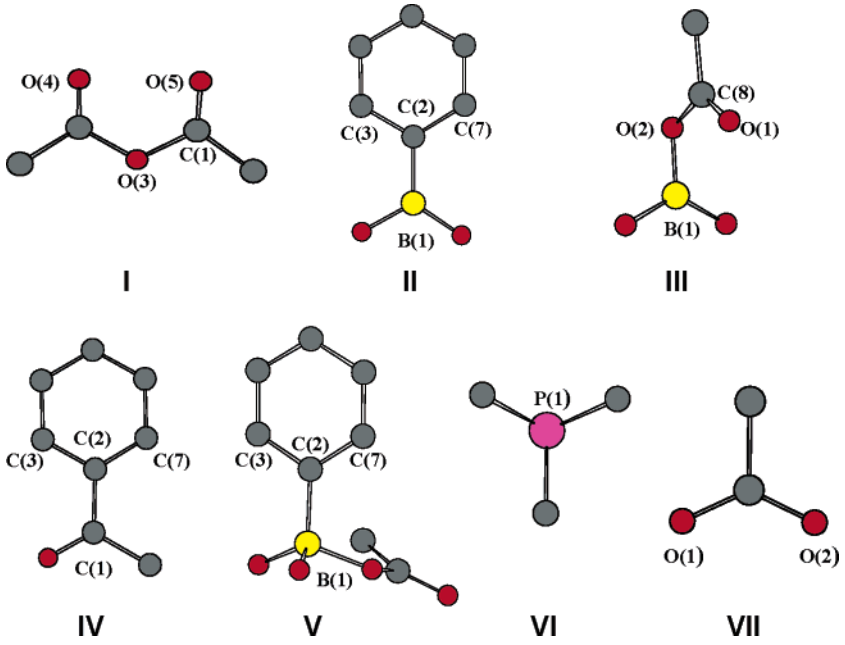

Figure 1. Starting materials and products involved in both pathways. BP86/6-31G* optimized structures are shown, with hydrogens removed for clarity. Color code: C gray, O red, B yellow, P violet.

3. Results

Figure 1 shows the starting materials and products of the reactions studied. For these molecules and all other relevant species, we optimized the geometry in the gas phase and calculated the electronic energy (E_e), the energy with zero-point vibrational corrections (E_0), the thermal enthalpy at 298 K (H_{298}), the Gibbs free energy at 298 K (G_{298}), and the energy with a continuum solvent model (E_{sov}), all at the BP86/6-31G* level of theory.

For each segment of the catalytic cycles, that is, oxidative addition, transmetalation, and reductive elimination, we evaluated the changes in electronic energy (ΔE_e) and Gibbs free energy (ΔG_{298}) for the optimized gas-phase geometries. The BP86/6-31G* results were validated by calculating single-point energies of the resulting intermediates and transition states with a larger basis set (ΔE_{EXT}). Finally, a solvent field was applied to account for bulk solvent effects (ΔE_{sov}). The figures that display energy profiles for reaction steps will show these four quantities.

A. Oxidative Addition and Ligand Exchange. A.1. Neutral Cycle. The classic catalytic cycle for a cross-coupling reaction starts from the coordinatively unsaturated palladium(0)-diphosphine d^{10}-complex **12**,[1] which has a linear geometry, with the methyl groups of the PMe_3 ligands in an eclipsed arrangement (Figure 2).[6,7] Oxidative addition of acetic anhydride directly leads to the cis-configured complex **13** ($\Delta E_e = -9.8$ kcal/mol, $\Delta G_{298} = 6.2$ kcal/mol). Only moderate activation ($\Delta E_e = 4.4$ kcal/mol, $\Delta G_{298} = 19.7$ kcal/mol) is required to reach the transition state **[12−13]‡**. In this transition state, the palladium is already in a four-coordinate, planar environment; the C(1)−O(4) distance of the acetic anhydride is elongated by 0.194 Å, and the imaginary mode ($92i$ cm^{-1}) involves further stretching of the C(1)−O(4) bond. The resulting intermediate **13** has a square-planar coordination, with the phosphine trans to the acyl group being more distant from Pd than the other one (Pd(1)−P(1) = 2.483 Å, Pd(1)−P(2) = 2.292 Å). This is as expected since the acyl group has a significantly stronger trans-effect than the acetyl group.[24] The oxidative nature of the addition reaction is obvious from the decrease of the NPA charge on Pd(1) by 0.311 *e* in going from **12** to **13**.

Despite several attempts, we did not find any energetically feasible pathway for an oxidative addition leading directly to a trans-configured palladium(II) complex. The fact that products isolated from oxidative addition reactions are usually trans-configured does not disprove that cis-complexes, such as **13**, are formed initially. Espinet et al. observed experimentally that the oxidative addition of aryl halides to palladium(0) complexes initially leads to cis-complexes, which in the absence of further reagents, slowly rearrange to the trans-isomers.[25]

There has been a long-standing debate about the most plausible starting point for the ensuing transmetalation step.[26] The main question is whether transmetalation can occur with two phosphines coordinated to the palladium center, or whether dissociation of one phosphine is required.[25,27] The observation that transmetalation of organoboron compounds can be inhibited by adding excess phosphine suggests such a dissociative mechanism. For organotin compounds, kinetic investigations by Hartwig and co-workers give further evidence for a reaction channel in which the phosphine dissociates prior to the transmetalation step.[28] Our results also support a dissociative mechanism, In careful searches starting from various different geometries, we were unable to identify a reaction pathway for the addition of phenylboronic acid to palladium(II)diphosphine compounds, such as **13**.[27] In contrast, we found several possible

(24) (a) Basolo, F.; Pearson, G. *Mechanism of Inorganic Reactions*, 2nd ed.; Wiley: New York, 1967. (b) Huheey, J. E.; Keiter, E. A.; Keiter, R. L. *Inorganic Chemistry: Principles of Structures and Reactivity*, 4th ed.; Harper-Collins College Publishers: New York, 1993.
(25) (a) Casado, A. L.; Espinet, P. *J. Am. Chem. Soc.* **1998**, *120*, 8978. (b) Casado, A. L.; Espinet, P. *Organometallics* **1998**, *17*, 954. (c) Espinet, P.; Echavarren, A. M. *Angew. Chem., Int. Ed.* **2004**, *43*, 4704. (d) Casares, J. A.; Espinet, P.; Salas, G. *Chem.—Eur. J.* **2002**, *8*, 4843.
(26) Miyaura, N. *J. Organomet. Chem.* **2002**, *653*, 54 and references therein.
(27) Napolitano, E.; Farina, V.; Persico, M. *Organometallics* **2003**, *22*, 4030 and references therein.
(28) Louie, J.; Hartwig, J. F. *J. Am. Chem. Soc.* **1995**, *117*, 11598.

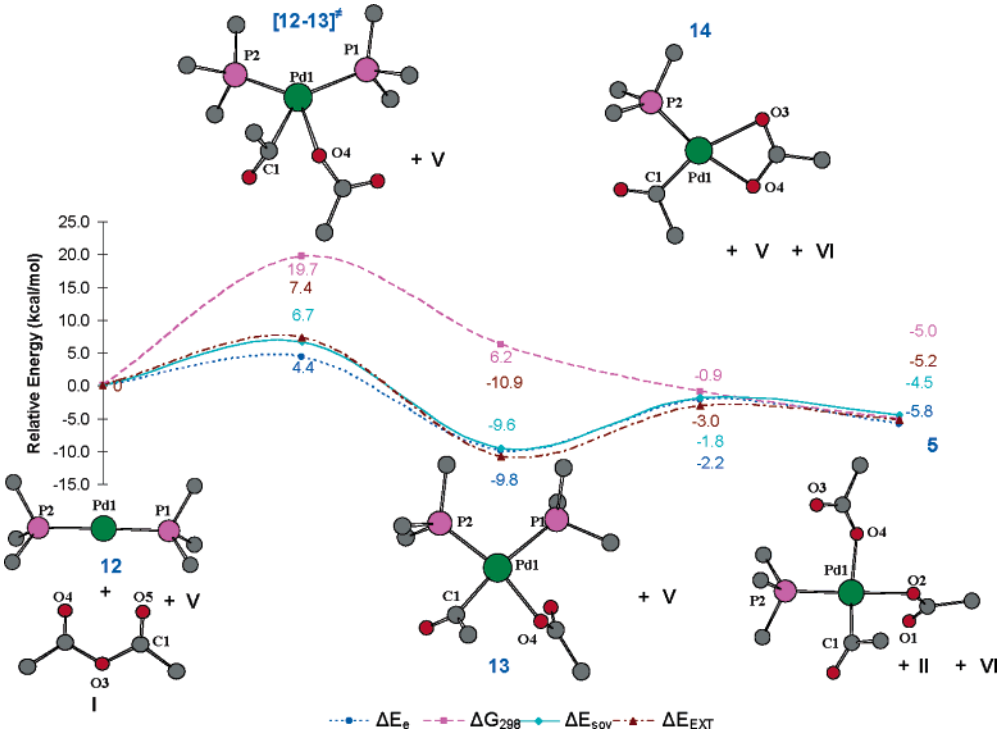

Figure 2. Energy profile for oxidative addition and ligand exchange: neutral pathway starting from $Pd(PMe_3)_2$ (**12**). Conventions see Figure 1.

reaction channels for the transmetalation of palladium(II)-monophosphine complexes, the most favorable of them starting from the anionic complex **5**. Therefore, additional steps had to be considered that transform the initial addition product **13** into **5**.

Our calculations showed that the most favorable pathway for the exchange of one of the phosphine ligands of **13** begins with the dissociation of the more distant phosphine under formation of **14**. In this intermediate, the acetate is coordinated to the palladium in a bidentate fashion with Pd(1)−O(4) and Pd(1)−O(3) bond distances of 2.179 and 2.310 Å, respectively. Due to this bidentate coordination of the acetate, the step is only slightly endothermic, and the increased entropy makes it exergonic (ΔE_e = 7.7 kcal/mol, ΔG_{298} = −7.1 kcal/mol).

In principle, intermediate **14** could serve as a starting point for a transmetalation reaction with the hypervalent boron species $[PhB(OH)_2OAc]^-$ (**V**) similar to that proposed by Miyaura and Suzuki for base-assisted transmetalation reactions.[29] However, explorations of such pathways indicate substantial barriers that are around 15 kcal/mol higher than those discussed below. This is probably related to the fact that the transfer of the acetate from **V** to **14** is calculated to be exergonic, so that at least in the gas phase, it is energetically more favorable to first transfer the acetyl group of compound **V** to the palladium under formation of intermediate **5** (ΔE_e = −3.6 kcal/mol, ΔG_{298} = −4.1 kcal/mol) prior to the transmetalation. Therefore, the transmetalation of **14** and **V** was not considered further.

The reaction step **14** → **5** is extremely exothermic (by more than 30 kcal/mol) if free acetate is used, with almost no activation barrier involved (ΔE_e < 3 kcal/mol). However, we consider it more reasonable to assume that the acetate will coordinate to the Lewis-acidic boronic acid whenever it is liberated within the reaction cycle, and we therefore chose to generate **5** from **14** by acetyl transfer from **V** (see Figure 2). Compound **5** is our favored starting point for the transmetalation. However, alternative pathways cannot yet be completely ruled out and remain under investigation.

Table 1. Optimized Geometric Parameters for Complexes **12** to **14** (bond distances are given in angstroms and bond angles in degrees)

No.	Pd–P(1)	Pd–P(2)	Pd–C(1)	Pd–O(4)	Pd–O(3)	P–Pd–P
12	2.922	2.991				178.6
[12−13]‡	2.441	2.280	2.215	2.344	3.639	122.9
13	2.483	2.292	2.048	2.164	3.005	102.3
14		2.272	1.988	2.179	2.310	

Basis set extension has only a very minor effect on the calculated reaction profile (ΔE_{EXT} vs ΔE_e, Figure 2), and the relative energies calculated for THF as the solvent using the CPCM model also show very similar trends as those in the gas phase. We have also performed such additional calculations for all subsequent reaction steps (see Figures 2−7). However, we will not further comment on them unless they differ significantly from the standard gas-phase BP86/6-31G* results.

Within the overall oxidative addition pathway, the initial addition of the anhydride to the palladium catalyst is generally expected to be rate-determining under the standard experimental conditions.[12] The computed activation barrier for this step is rather low, partly because we have chosen to use the small and electron-rich trimethylphosphine ligand in the calculations (rather than triarylphosphines).

Selected structural parameters of all intermediates and transition states of the oxidative addition/ligand exchange sequence are summarized in Table 1. Selected NPA charges, dipole moments (Table S3), and more detailed structural data are available in the Supporting Information.

A.2. Anionic Cycle. An alternative catalytic pathway for the oxidative addition was sought starting from the $[Pd(PMe_3)_2OAc]^-$

(29) Moriya, T.; Miyaura, N.; Suzuki, A. *Synlett* **1994**, 149.

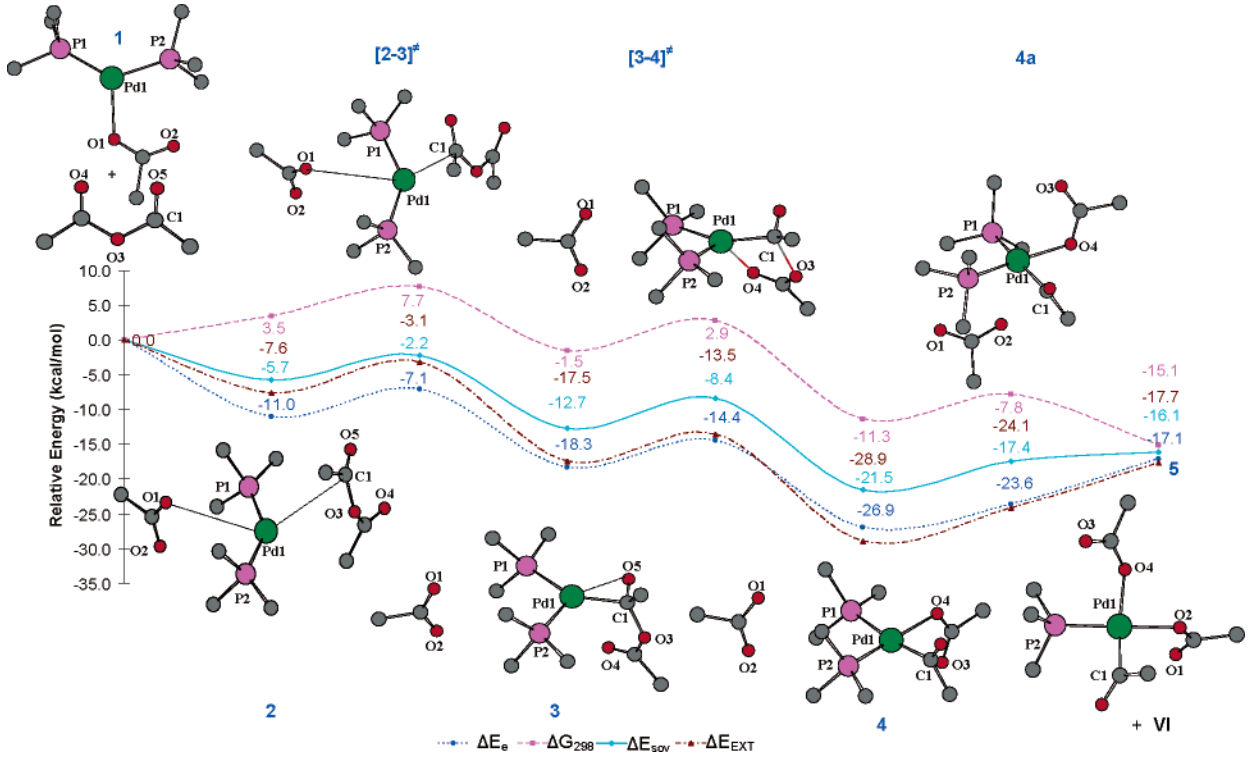

Figure 3. Energy profile for oxidative addition and ligand exchange: anionic pathway starting from $[Pd(PMe_3)_2OAc]^-$. Conventions see Figure 1.

(**1**) complex to determine whether such "Jutand-type" anionic palladium(0) species would give rise to a more favorable overall mechanism. According to Amatore and Jutand, an oxidative addition to such anionic species should result in the formation of five-coordinate palladium(II) species.[5] However, in analogy to our theoretical studies on the oxidative addition of aryl halides,[6] we did not find any evidence for the existence of such intermediates. Instead, upon bringing acetic anhydride (**I**) into the proximity of the anionic palladium(0) catalyst **1**, the van der Waals adduct **2** is formed in a barrierless reaction. In this species, the electron-poor carbonyl carbon of the incoming acetic anhydride interacts with the electron-rich palladium center ($\Delta E_e = -11.0$ kcal/mol, $\Delta G_{298} = 3.5$ kcal/mol, $\Delta E_{sov} = -5.7$ kcal/mol). While palladium is calculated to be almost neutral (0.004 *e*) in **1**, it has a negative charge of −0.244 *e* in complex **2** (Table S3), mostly due to charge transfer from the two phosphine ligands, which allows for an attractive electrostatic interaction with the positively charged carboxylic carbon C(1) (0.802 *e*).

Intermediate **2** has an almost planar geometry around palladium, with the acetate and the anhydride residues oriented perpendicular to the P−Pd−P plane. Compared to **1**, the Pd−O(1) distance is significantly increased (Pd(1)−O(1) = 4.183 Å in **2** vs 2.327 Å in **1**), and the P−Pd−P bond angle has widened by more than 10 (Figure 3). The Pd(1)−C(1) distance of 3.735 Å is quite large, but already within the range of a weak interaction. Two hydrogen atoms of the anhydride appear to interact with the palladium center (Pd−H_1 = 2.626 Å, Pd−H_2 = 2.519 Å, C−H_1 = 1.118 Å, C−H_2 = 1.122 Å) causing a slight distortion of the coordination geometry.

Starting from compound **2**, the oxidative addition proceeds in two steps. In an exergonic reaction ($\Delta E_e = -7.3$ kcal/mol, $\Delta G_{298} = -4.8$ kcal/mol), intermediate **3** is formed via an energetically low-lying transition state **[2−3]**‡ ($\Delta E_e = 3.9$ kcal/mol, $\Delta G_{298} = 4.2$ kcal/mol, confirmed by IRC calculations), with an imaginary frequency mode (52*i* cm^{-1}) that reflects the gradual approach of C(1) toward the palladium center. In intermediate **3**, the anhydride is bound by a η^2−type interaction between the C(1)−O(5) carbonyl double bond and the palladium (Pd(1)−C(1) = 2.085 Å, Pd(1)−O(5) = 2.216 Å), the C(1)−O(5) bond being elongated from 1.209 Å in **I** to 1.285 Å in **3**. The second carboxylic oxygen O(4) of the anhydride is almost in an axial position with respect to the metal center, with a distance (Pd(1)−O(4) = 2.929 Å) that allows for a weak interaction. In contrast, the acetate ligand is far away from the metal center (Pd(1)−O(1) = 5.143 Å) and acts as a weakly bound spectator ligand.

During the transition from **2** via **[2−3]**‡ to **3**, there are significant changes in the atomic charges of palladium and of the carboxy group, indicating that this reaction is already part of the oxidative addition. Almost 0.5 *e* are transferred from the metal center (Pd(1) = −0.244 *e* in **2**, Pd(1) = 0.241 *e* in **3**) to the carboxy group (C(1) = 0.802 *e* in **2**, C(1) = 0.458 *e* in **3**; O(5) = −0.544 *e* in **2**, O(5) = −0.642 *e* in **3**).

In the next step, the bond between C(1) and O(3) in **3** is broken to form the oxidative addition product **4** via the transition state **[3−4]**‡, and further electron density is transferred from the metal and the phosphine ligands to C(1) and O(4) (C(1) = 0.458 *e* in **3** and 0.381 *e* in **4**; O(4) = −0.585 *e* in **3** and −0.706 *e* in **4**) but not to O(5) (O(5) = −0.527 *e* in **4**).

The transition state **[3−4]**‡ contains a five-membered ring in which O(4) approaches palladium from an axial direction. The imaginary mode (106*i* cm^{-1}) involves this approach of O(4) with simultaneous C(1)−O(3) bond breaking. At the same time, the Pd(1)−C(1) bond is shortened, while the Pd(1)−O(5) distance increases (change from η^2 to η^1 coordination, reinstating the double bond character between C(1) and O(5)). The activation energy for the formation of the cis-configured complex **4** is low ($\Delta E_e = 3.9$ kcal/mol, $\Delta G_{298} = 4.4$ kcal/mol),

Table 2. Optimized Geometric Parameters for Complexes **1** to **5** (bond distances are given in angstroms and bond angles in degrees)

No.	Pd–P(1)	Pd–P(2)	Pd–C(1)	Pd–O(1)	Pd–O(2)	Pd–O(4)	Pd–O(5)	P–Pd–P
1	2.247	2.307		2.327	3.535			132.2
2	2.291	2.299	3.735	4.183	4.218	5.006	1.214	142.6
[2−3]‡	2.314	2.317	2.590	4.233	4.267	4.512	1.223	140.3
3	2.403	2.297	2.085	5.143	5.144	2.929	1.285	105.2
[3−4]‡	2.433	2.291	2.047	5.115	5.195	2.454	1.248	104.3
4	2.484	2.308	2.031	5.191	5.338	2.184	1.223	99.7
4a	2.459	2.285	2.031	4.226	3.162	2.195	1.227	103.7
5		2.274	1.997	3.059	2.147	2.215	1.231	

and the overall reaction from **3** to **4** is exergonic ($\Delta E_e = -8.6$ kcal/mol, $\Delta G_{298} = -9.8$ kcal/mol).

As in the case of the neutral pathway, an alternative mechanism leading to the corresponding trans-complex was not found, and all attempts failed to accomplish a transmetalation starting from a diphosphine complex (i.e., **4** or **4a**). However, the replacement of one of the phosphine ligands by acetate is easily achieved. Internal rotation around the Pd(1)−O(4) bond in **4** leads to a less stable conformer **4a**, where the orientation of the bound acetate ligand is more suitable for the substitution of a phosphine ligand by the spectator acetate ligand (Figure 3). In contrast to **4**, the oxygen atom O(3) is at the opposite side of the spectator acetate ligand and thereby facilitates its approach in **4a**. Gradual removal of any one of the two phosphines from **4a** prompts the spectator acetate ligand to coordinate to the palladium replacing the phosphine. The representation in Figure 3 is slightly simplified as this substitution involves additional intermediates.[30]

Since the Pd(1)−P(1) bond is weaker than the Pd(1)−P(2) bond, the P(1)Me_3 ligand is displaced, and an intermediate **5** is formed in which the two acetate groups are oriented cis to each other. This requires less activation energy ($\Delta E_e = 8.5$ kcal/mol, $\Delta G_{298} = 7.5$ kcal/mol) than the alternative formation of the *trans*-diacetate complex, as the removal of the other phosphine P(2)Me_3 from **4a** would be more endothermic ($\Delta E_e = 12.9$ kcal/mol, $\Delta G_{298} = 11.5$ kcal/mol).

The structural parameters of all intermediates and transition states of the anionic pathway are summarized in Table 2. Selected NPA charges, dipole moments (Table S4), and more detailed structural data are available in the Supporting Information.

Overall, we have identified valid reaction pathways for the oxidative addition of acetic anhydride to both a neutral and an anionic palladium(0) species. For both pathways, the calculated energy profiles seem reasonable (Figures 2 and 3). Although one has to be careful when comparing the energies of the two pathways with each other (see Discussion in section 4), our results suggest that the anionic pathway for the oxidative addition is energetically more favorable than the neutral one. Starting from the anionic species **1**, the highest free-energy barrier ($\Delta G_{298} = 7.7$ kcal/mol) of the oxidative addition sequence is found to be significantly lower than that of the neutral pathway ($\Delta G_{298} = 19.7$ kcal/mol). This is consistent with the experimental finding that catalysts generated in situ from palladium(II)acetate show a higher activity than preformed palladium(0)phosphine complexes.[5]

B. Transmetalation. As mentioned earlier, all our attempts to identify a transmetalation pathway starting from diphosphine complexes failed. For example, approaching phenylboronic acid to **13** from various angles resulted in high energies and ultimate dissociation of one of the phosphines. The same outcome was observed when starting from the corresponding trans-configured complex, $[Pd(PMe_3)_2(OAc)(COMe)]^-$.[31] In contrast, several plausible pathways for transmetalation reactions of monophosphine complexes, such as **5**, were found.

While optimizing the geometry of compound **5**, we discovered an energetically almost degenerate rotamer **5a**, which proved to be more suitable for the following reaction. In **5a**, the two sp^2-hybridized oxygen atoms of the acetyl groups (O(3) and O(1)) are pointing out of the coordination plane into the same direction, while they are on opposite sides in intermediate **5**.

Bringing a molecule of boronic acid $PhB(OH)_2$ (**II**) closer to the palladium center of **5a** affords the stable adduct **6** in a barrierless reaction. In this precoordination complex, one OH group of the boronic acid forms a hydrogen bond to O(4), which carries the most negative charge of all oxygen atoms (O(4) = −0.781 *e*, O(3) = −0.679 *e*, O(2) = −0.732 *e*, and O(1) = −0.665 *e*). The bridging hydrogen bond is responsible for the high stability of **6** in comparison to **5a** and $PhB(OH)_2$ ($\Delta E_e = -19.7$ kcal/mol, $\Delta G_{298} = -4.6$ kcal/mol). Consequently, a deep valley interrupts the smooth energy profile of the reaction, causing a high-energy barrier for the following step. It should be stressed, however, that these results come from gas-phase calculations and do not reflect the situation in solution where the boronic acid will form hydrogen bonds either to a reaction partner (as in **6**) or to an external partner, such as a solvent molecule. In our gas-phase model calculations, the former are included, but the latter are not. For a realistic assessment of the situation in solution, these interactions with an external partner should be taken into account. On the basis of calculations on model systems consisting of water, THF, and boronic acid, the energy arising from a hydrogen bond between the boronic acid and a solvent molecule was estimated to be around −10 kcal/mol (ΔE_e).[32] Subtracting this value from the calculated relative energy of **6** (−37.5 kcal/mol; Figure 4) leads to a much smoother and, as we think, much more realistic reaction profile. For the same reason, −20 kcal/mol will be subtracted from the calculated value of −40.8 kcal/mol in intermediate **8**, with its two internal hydrogen bonds.

The conversion of intermediate **6** into intermediate **7** is decisive within the transmetalation process since it involves the first direct coordination of the phenyl group to the palladium,

(30) The reaction channel from **4a** to **5** involves a transition state **[4a-4b]‡** leading to a van der Waals adduct **4b** with loosely bound PMe_3 and acetate ligands, followed by complete removal of PMe_3 to yield another van der Waals adduct **4c**, and subsequent coordination of acetate to generate **5**. The corresponding data are included in the Supporting Information.

(31) Goossen, L. J.; Koley, D.; Hermann, H.; Thiel, W. Manuscript in preparation.

(32) ΔE_e values for BOH−THF and BOH−OH_2 hydrogen bonds were calculated to be −9.4 and −10.7 kcal/mol, respectively. See the Supporting Information for details.

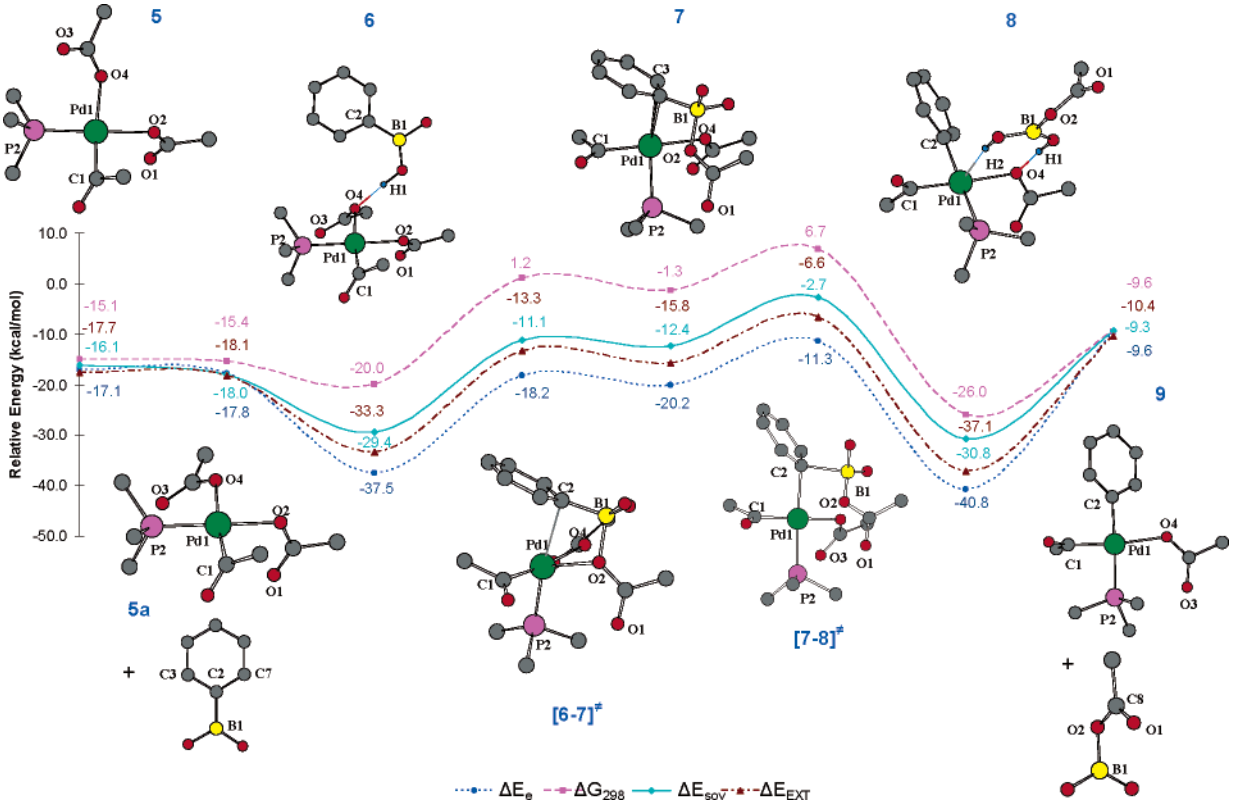

Figure 4. Energy profile for the transmetalation reaction involving intermediates **5** to **9**. Relative energies are given with respect to the anionic pathway (Figure 3). Conventions see Figure 1.

initially by an η^2 bond to the C(2)−C(3) bond. We have located the corresponding transition state **[6−7]**‡ and confirmed by IRC calculations that it connects **6** and **7**. It contains a four-membered ring formed by the atoms Pd(1), C(2), B(1) of the boronic acid, and O(2) of the acetate ligand. The imaginary mode (40*i* cm^{-1}) shows the simultaneous approach of the phenyl group toward the palladium along with an elongation of the O(2)−Pd(1) bond. Similar four-membered cyclic transition states have been postulated for other palladium-catalyzed reactions. For example, Napolitano et al. found a cyclic transition state for the transmetalation in a B3LYP/LANL2DZ calculation performed on Stille couplings,[27] and Matos et al. proposed a similar geometry for the transfer of alkyl groups from alkylboranes to palladium complexes on the basis of NMR studies.[33] Our computed transmetalation mechanism is consistent with experimental work performed by Miyaura, who suggested that transmetalation with oxo-palladium(II) complexes may involve a rate-determining coordination of the RO (R = COMe) ligand to the boron atom.[29]

In the complex **7**, the phenyl group is coordinated via an η^2 bond, as can be seen by the short palladium−carbon distances (Pd(1)−C(2) = 2.549 Å and Pd(1)−C(3) = 2.448 Å) and the increase in the C(2)−C(3) bond distance (1.432 Å in **7** vs 1.414 Å in $PhB(OH)_2$) (Figure 4). The formation of η^2 π-complexes, such as **7**, preceding the insertion of a transition metal into an aryl−X bond is not uncommon in palladium chemistry. For example, such intermediates were also found in oxidative addition reactions of aryl halides with palladium(0) complexes,[8,11,34] the calculated intermediates structurally resembling intermediate **7**.

Gradual elongation of the C(2)−B bond of **7** leads to intermediate **8**, in which the C(2)−B bond is cleaved. The transition state **[7−8]**‡ (confirmed by IRC) reveals an elongated carbon−boron bond (C(2)−B = 2.122 Å in **[7−8]**‡ and 1.663 Å in **7**). The imaginary mode (254*i* cm^{-1}) indicates a stretching of the C(2)−B(1) bond in the transition state. The activation barrier is moderate (ΔE_e = 8.8 kcal/mol, ΔG_{298} = 8.0 kcal/mol).

A hydrogen-bonding stabilization similar to that observed in intermediate **6** is seen in **8**, giving rise to a very low energy of this intermediate. Again, this effect is expected to be much less pronounced under experimental conditions, where all species are solvated. Removal of the borate leads to the square-planar intermediate **9**, in which the phenyl and acetyl groups are oriented cis to each other. Hence, the reductive elimination can proceed directly from **9**, without any requirement of further isomerization.

The structural parameters of all intermediates and transition states of the common transmetalation step are summarized in Table 3. Selected NPA charges, dipole moments (Table S5), and more detailed structural data are available in the Supporting Information.

C. Reductive Elimination. The traditional mechanism for cross-coupling reactions has been derived from the known geometries of isolable palladium complexes and, thus, involves trans-configured palladium(II)diphosphine species as intermediates (Scheme 2). One of the strongest arguments against this proposed mechanism is that the reductive elimination of the cross-coupling products $Pd(PR'_3)_2RAr$ from a trans-configured diphosphine intermediate would require an additional cis−trans

(33) Matos, K.; Sonderquist, J. A. *J. Org. Chem.* **1998**, *63*, 461.

(34) Senn, H. M.; Ziegler, T. *Organometallics* **2004**, *23*, 2980.

Table 3. Optimized Geometric Parameters for Complexes **5a** to **9** (bond distances are given in angstroms and bond angles in degrees)

No.	Pd–P(2)	Pd–C(1)	Pd–O(2)	Pd–O(4)	Pd–C(2)	C(2)–B1	C(1)–Pd–P(2)
5a	2.281	1.989	2.150	2.203			
6	2.285	1.981	2.129	2.267	5.446	1.586	90.7
[6−7]‡	2.293	1.979	2.486	2.238	2.817	1.654	89.6
7	2.315	1.987	3.066	2.231	2.549	1.663	86.8
[7−8]‡	2.317	1.983	2.794	2.259	2.245	2.122	88.3
8	2.383	1.989	5.372	2.253	2.076	4.686	91.8
9	2.395	1.987	–	2.232	2.086	–	91.5

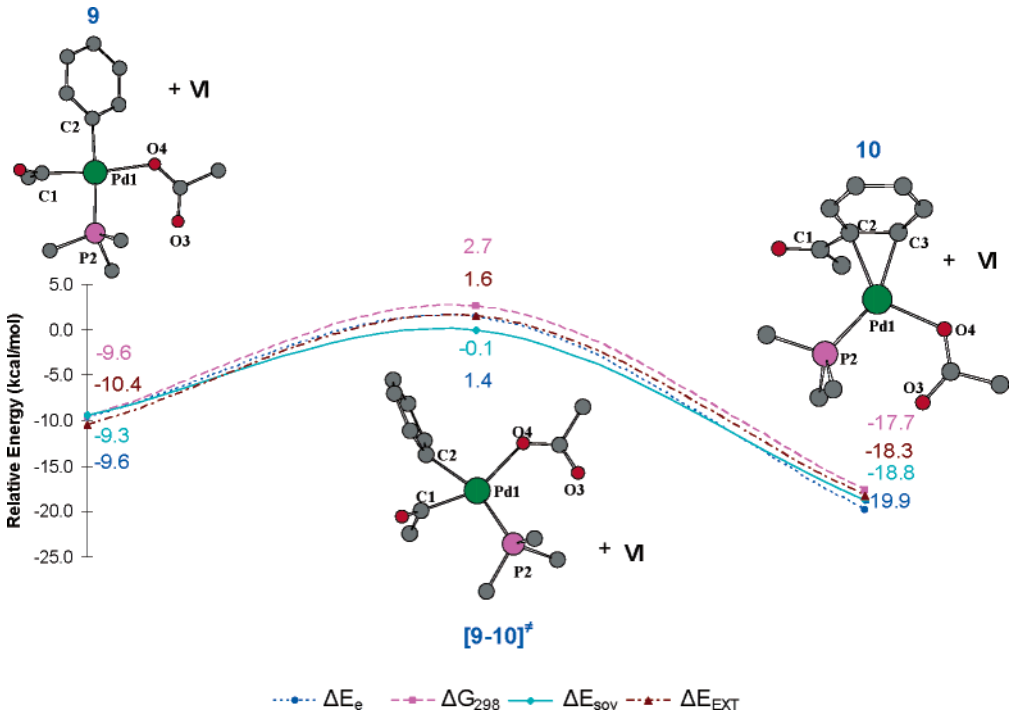

Figure 5. Energy profile from intermediate **9** to **10**. Conventions see Figures 1 and 4.

isomerization, which can be expected to be strongly endothermic. Amatore and Jutand have pointed out that if this mechanism were true, the isomerization step should be rate-determining.[5] Since this is in contrast to experimental findings, they went on to propose their alternative catalytic cycle involving five-coordinate palladium complexes (Scheme 2).

According to our calculated mechanism, which does not invoke any five-coordinate intermediates, the acyl and phenyl groups are already positioned cis to each other in the intermediate **9**, which is set up for reductive elimination. Due to the close proximity of these groups, the reductive elimination of the product acetophenone proceeds smoothly, as expected from experimental findings.

We calculated two possible pathways for this final step in the catalytic cycle, one giving rise to the neutral $Pd(PMe_3)_2$ species (**12**), and the other one reinstating the anionic $[Pd(PMe_3)_2OAc]^-$ (**1**) complex. In both cases, starting from **9**, reductive elimination is initiated by the formation of a bond between the aryl and the acyl group, leading to a η^2 π-complex of palladium with acetophenone (**10**). In the corresponding transition state **[9−10]‡** (ΔE_e = 11.0 kcal/mol, ΔG_{298} = 12.2 kcal/mol), the C(1)−C(2) distance is already reduced to 1.965 Å, and the imaginary mode (280*i* cm^{-1}) indicates a further shortening of this distance. The Pd(1)−P(2) bond length in **[9−10]‡** is reduced by 0.097 Å, which may arise from the fact that the phenyl group is no longer positioned trans to the phosphine ligand.

We also tested whether the approach of a second PMe_3 ligand to compound **9** would give rise to an alternative pathway for the reductive elimination of acetophenone but found that, in this case, the other phosphine, not the acetate or the acetophenone, left the coordination sphere of the palladium.

In the relatively stable intermediate **10** (ΔE_e = −10.3 kcal/mol, ΔG_{298} = −8.2 kcal/mol with respect to **9**), the phenyl moiety of the newly formed acetophenone remains closely bound to the palladium via an η^2 coordination of the aromatic double bond adjacent to the acyl group (C(2)−Pd(1) = 2.226 Å and C(3)−Pd(1) = 2.205 Å; Figure 5).

C.1. Neutral Cycle. To complete the catalytic cycle, the coordinated acetophenone has to be released from complex **10**, and the $Pd(PMe_3)_2$ species **12** has to be regenerated. Although this process requires several steps, they are all energetically very similar and involve only negligible activation barriers. As before, the $[PhB(OH)_2OAc]^-$ species is used as a carrier for the acetate anion, which is transferred back to the palladium in step **10** → **15**. In this way, unrealistically high barriers are avoided, and one obtains a more accurate view on the relative energies of the intermediates within the catalytic cycle. Under the authentic reaction conditions used in the catalysis, the acetate probably coordinates not only to the boron species in solution but also to the polar solvent. Therefore, such ligand-exchange reactions are difficult only in gas-phase calculations, while they should be facile in solution. Coordination of the boronic acid to the most electronegative oxygen of the acetate ligand results in the

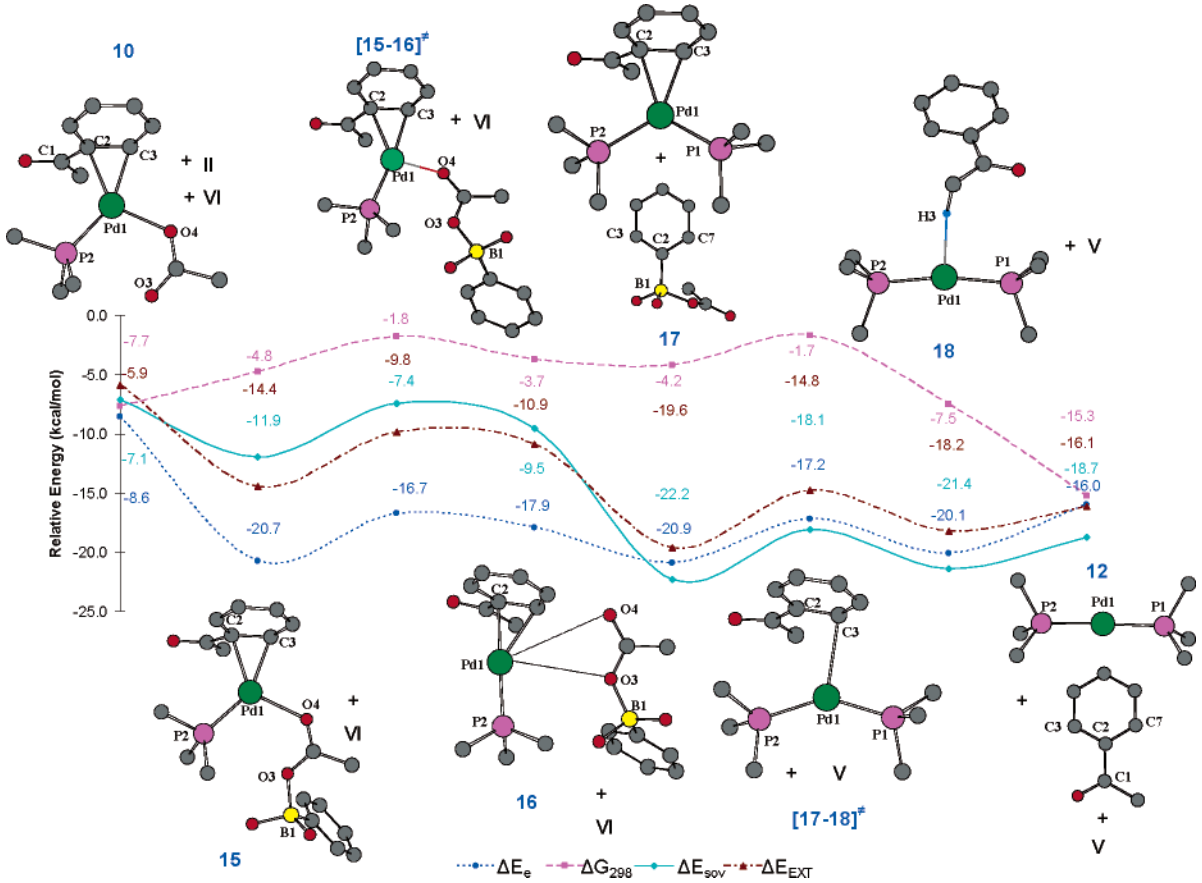

Figure 6. Energy profile for reductive elimination reaction involving the liberation of acetophenone and the regeneration of the neutral complex **12**. Relative energies are given with respect to the neutral pathway (Figure 2). Conventions see Figure 1.

Table 4. Optimized Geometric Parameters for Complexes Involved during Reductive Elimination (bond distances are given in angstroms and bond angles in degrees)

No.	Pd–P(1)	Pd–P(2)	Pd–C(2)	Pd–O(4)	Pd–O(3)	P–Pd–P	P(2)–Pd–O(4)
9		2.395	2.086	2.232	3.578		96.5
[9−10]‡		2.298	2.185	2.258	3.549		102.7
10		2.313	2.226	2.231	3.398		107.5
15		2.323	2.231	2.323	3.369		112.4
[15−16]‡		2.291	2.302	3.095	3.596		113.8
16		2.277	2.215	4.761	4.437		112.8
17	2.337	2.367	2.309			117.8	
[17−18]‡	2.294	2.335	3.116			144.9	
18	2.289	2.317	4.975			169.6	

formation of the intermediate **15**, in which the Pd(1)−O(4) bond distance is larger than that in **10** (2.323 vs 2.231 Å). Starting from this complex, the decoordination of the anionic boron species **V** does not require much energy, and the gradual elongation of Pd(1)−O(4) bond results in the formation of an adduct **16**, where the Pd(1)−O(4) distance is as long as 4.761 Å. Reaching the corresponding transition state **[15−16]‡**, which has a Pd(1)−O(4) distance of 3.095 Å, requires only little activation (ΔE_e = 4.0 kcal/mol, ΔG_{298} = 3.0 kcal/mol). If a phosphine is brought close to this coordinatively unsaturated complex, it immediately binds to the palladium, while the $[PhB(OH)_2OAc]^-$ species completely leaves the coordination sphere.

Due to the strong electron-donating ability of the phosphine, the ligand exchange (**16** → **17**) causes a loosening of the coordination of the acetophenone (C(2)−Pd(1) = 2.309 Å, C(3)−Pd(1) = 2.300 Å). As a result, the subsequent removal of the phenyl group from **17** easily cleaves the Pd−C bond via the transition state **[17−18]‡**. The imaginary mode (40*i* cm^{-1}) involves the movement of the phenyl group away from the metal center. Interestingly, the acetophenone does not fully dissociate but remains loosely bound to **18** via one of the hydrogens (Pd(1)−H(3) = 2.353 Å, Figure 6). Such a weak interaction may survive in the gas phase, but most probably not in a coordinating solvent. Although, surprisingly, many steps are required to regenerate the initial $Pd(PMe_3)_2$ species **12**, due to energetically low-lying intermediates, the entire sequence should be facile as it does not require much activation (Figure 6).

The structural parameters of all intermediates and transition states of the neutral pathway of the reductive elimination/ligand exchange sequence are summarized in Table 4. Selected NPA charges, dipole moments (Table S6), and more detailed structural data are available in the Supporting Information.

C.2. Anionic Cycle. We also calculated an alternative route for the reductive elimination leading to the anionic species, $[Pd(PMe_3)_2OAc]^-$ (**1**), to resume the second catalytic cycle.

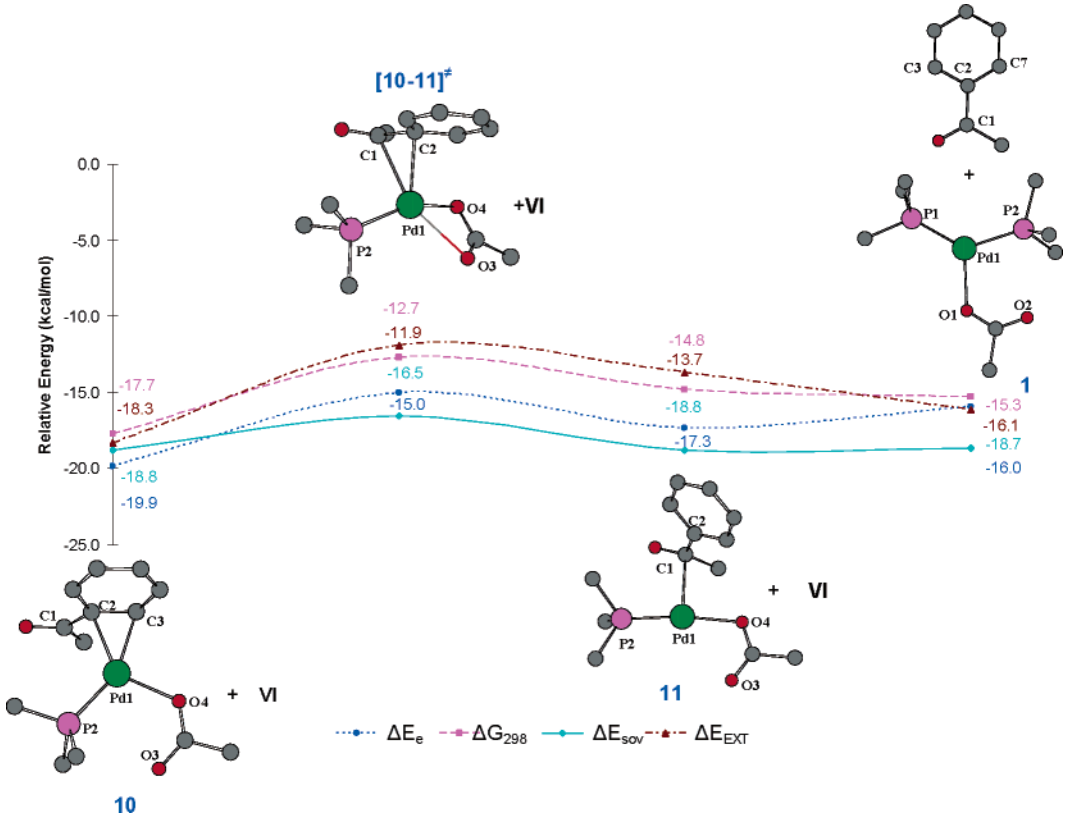

Figure 7. Energy profile for reductive elimination reaction involving the liberation of acetophenone and the regeneration of the anionic complex **1**. Conventions see Figure 1.

When approaching an additional phosphine to **10**, a simple exchange with the other phosphine is observed. In contrast, the removal of the phenyl group from **10** by gradually increasing the Pd(1)−C(2) bond length results in the formation of the adduct **11** via the low-energy transition state **[10−11]**‡ (ΔE_e = 4.9 kcal/mol, ΔG_{298} = 5.0 kcal/mol). In intermediate **11**, the acetophenone remains loosely bound to the palladium by an interaction between the electron-poor C(1) and the nucleophilic, electron-rich palladium center (Figure 7).

In **11**, the charge on C(1) is reduced to 0.419 *e*, as a consequence of the interaction with the palladium. The imaginary frequency (69*i* cm^{-1}) of the transition state **[10−11]**‡ reflects the concomitant elongation of the Pd(1)−C(2) bond and the formation of the Pd(1)−C(1) bond. In **[10−11]**‡, the acetate is coordinated to the metal center in a bidentate manner (Pd(1)−O(4) = 2.422 Å, Pd(1)−O(3) = 2.559 Å). This bidentate character diminishes in intermediate **11**, which has one strong palladium−oxygen bond (Pd(1)−O(4) = 2.174 Å, Pd(1)−O(3) = 3.088 Å).

Bringing a phosphine molecule close to **11** results in the direct formation of the anionic species, $[Pd(PMe_3)_2OAc]^-$ (**1**), and the product acetophenone is liberated through a barrierless reaction step. Overall, this anionic path requires fewer steps but is energetically similar to the neutral pathway **15** → **12**.

The structural parameters of the transition state **[10−11]**‡ and intermediate **11** are summarized in Table 5. Selected NPA charges, dipole moments (Table S7), and more detailed structural data are available in the Supporting Information.

Table 5. Optimized Geometric Parameters for Complexes **[10−11]**‡ and **11** (bond distances are given in angstroms and bond angles in degrees)

No.	Pd–P(2)	Pd–C(2)	Pd–O(4)	Pd–O(3)	P(2)–Pd–O(4)
[10−11]‡	2.238	2.448	2.422	2.559	145.6
11	2.214	3.018	2.174	3.088	172.7

4. Discussion and Conclusion

In summary, two mechanistically and energetically plausible catalytic cycles for the cross-coupling of phenylboronic acid with acetic anhydride have been identified, using either the neutral $Pd(PMe_3)_2$ or the anionic $[Pd(PMe_3)_2OAc]^-$ complex as the starting point. According to our calculations, both the neutral and the anionic pathway give rise to cis-configured palladium(II)diphosphine intermediates (**13** and **4**) in the oxidative addition step. In the neutral case, this is not unexpected as an increasing amount of evidence supports initial formation of the cis-configured intermediates in oxidative addition reactions of palladium(0) complexes, before they slowly isomerize to the isolable but significantly less reactive trans-configured palladium(II)diphosphine complexes.

The existence of an anionic cycle starting from the three-coordinate intermediate $Pd(PMe_3)_2OAc]^-$ that was expected from the findings of Amatore and Jutand could be confirmed. However, we did not find any evidence for the intermediacy of five-coordinate species in our model reaction. Instead, our calculations suggest that the higher catalytic activity of anionic complexes, such as $[Pd(PMe_3)_2OAc]^-$, arises from their stronger ability to coordinate to carbon electrophiles. This results in an exothermic precoordination of the substrate, which pulls it into close proximity to the palladium center, thereby significantly lowering the activation barrier for the actual oxidative addition step.

For the transmetalation of boronic acids, the only identifiable pathway involves dissociation of one phosphine ligand from

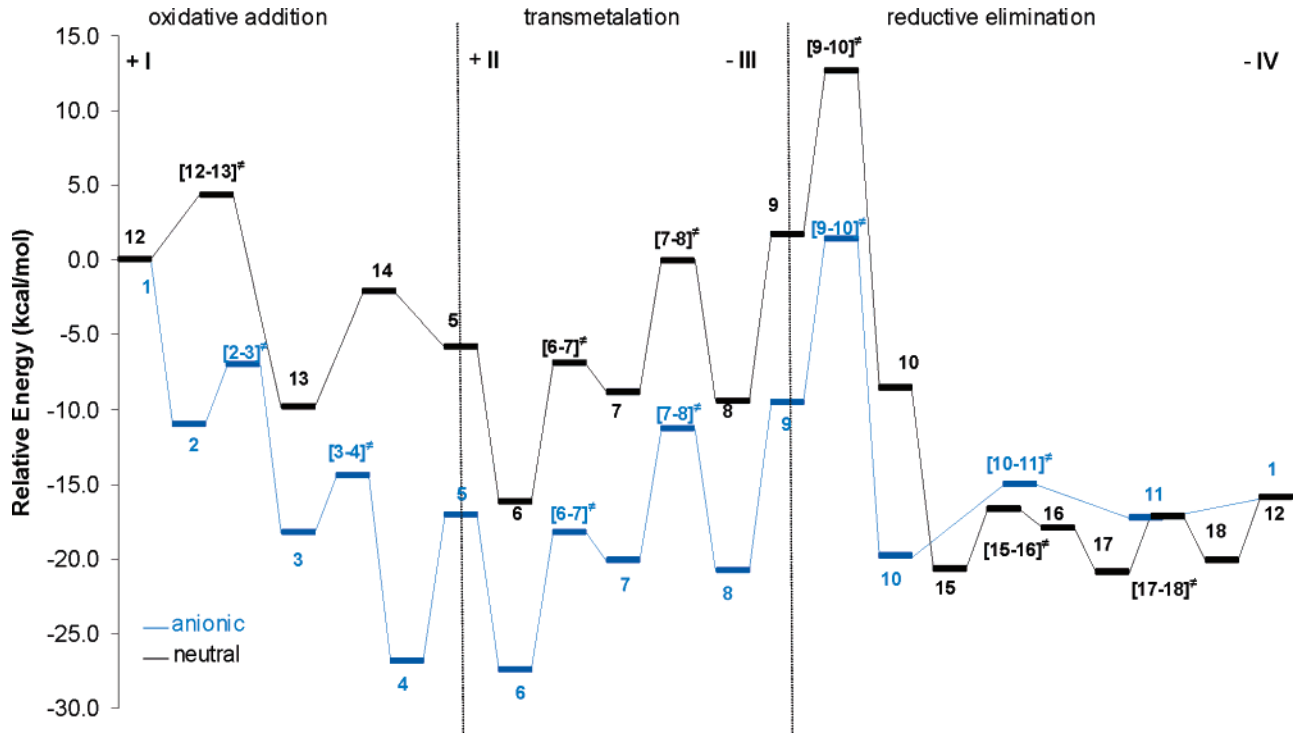

Figure 8. Relative energies (ΔE_e in kcal/mol) for the intermediates and transition states involved in the neutral (black) and anionic (blue) cycle. A reference value of 0 has been assigned to the reactants in both cases, and the values for **6** and **8** have been corrected by 10 kcal/mol per internal hydrogen bond (see text).

the palladium, while all attempts failed to initiate a transmetalation reaction starting from palladium(II)diphosphine intermediates. This result is consistent with experimental findings, indicating that the transfer of an organyl residue from stannates to palladium is retarded by the presence of excess phosphine.[28,35] It might be an additional reason the most active catalysts known for Suzuki couplings involve sterically extremely crowded phosphine ligands that preclude the formation of palladium diphosphine complexes.[36]

In view of the long-standing controversy over the role of the base in Suzuki couplings, it is worth mentioning that our calculations predict the base to coordinate both to boron and to palladium in the decisive transition state of the transmetalation.

For the reductive elimination, two possible pathways were again found, regenerating either a neutral (**12**) or an anionic species (**1**). Both pathways are energetically equally favorable, thus demonstrating how easily a crossover between the anionic and the neutral pathway could occur.

Figure 8 shows the energy profiles for both pathways relative to the reactants, which are defined to have zero energy in each case. As discussed in section 3B, a correction of 10 kcal/mol per internal hydrogen bond has been applied for **6** and **8** to avoid differential stabilizing effects that will operate only in the gas phase and not in solution. The top part of Figure 8 specifies the three phases of the catalytic cycle as well as the steps where the reactants are introduced (+**I**, +**II**) and where the products are liberated (−**III**, −**IV**).

(35) (a) Farina, V.; Krisnan, B. *J. Am. Chem. Soc.* **1991**, *113*, 9585. (b) Farina, V.; Roth, G. P. Recent Advances in the Stille Reaction. In *Adv. Metalorg. Chem.* **1996**, *5*, 1. (c) Amatore, C.; Bahsoun, A.; Jutand, A.; Meyer, G.; NdediNtepe, A.; Ricard, L. *J. Am. Chem. Soc.* **2003**, *125*, 4212.

(36) (a) Old, D. W.; Wolfe, J. P.; Buchwald, S. L. *J. Am. Chem. Soc.* **1998**, *120*, 9722. (b) Wolfe, J. P.; Buchwald, S. L. *Angew. Chem., Int. Ed.* **1999**, *38*, 2413.

At first sight, the largest barrier seems to be associated with the transformation **8** → **10** which, however, consists of two distinct steps: removal of borate **III** (**8** → **9**) followed by a rearrangement (**9** → **10**) that initiates the reductive elimination. In solution, intermediate **9** will equilibrate with the environment, and therefore, the two steps **8** → **9** and **9** → **10** will be kinetically distinct, each of them having a rather small barrier. Hence, in an overall view, all individual steps on the two pathways exhibit reasonably small barriers (<15 kcal/mol).

The transformation **5** → **10** is common to both pathways, and the two reaction profiles are therefore parallel in this region. The black curve for the neutral pathway is shifted by 11.3 kcal/mol relative to the blue one for the anionic pathway because the reactants have been chosen to be **I** + **II** + $Pd(PMe_3)_2$ (**12**) + $[PhB(OH)_2OAc]^-$ (**V**) in the former case, and **I** + **II** + $[Pd(PMe_3)_2OAc]^-$ (**1**) in the latter case; the difference of 11.3 kcal/mol is simply the calculated energy for the formal reaction **12** + **V** → **1** + **II** that connects the reactants. It is obvious that the relative position of the two curves depends on the choice of the model systems, that is, on the source of acetate (see section 3A); the formation of **1** is endothermic by 11.3 kcal/mol from **12** and **V**, but exothermic by 18.4 kcal/mol from **12** and free acetate. This implies that the relative preference for the neutral and anionic pathways will depend on the experimental conditions, that is, on the accessibility of acetate.

Figure 9 shows the free-energy profiles for both pathways using the same conventions as in Figure 8. The overall appearance of the curves in Figures 8 and 9 is rather similar, but there are also some notable differences. Association reactions (adding reactants in steps **1** → **3**, **12** → **13**, and **5** → **6**) suffer from an entropic penalty because of the loss of translational and rotational degrees of freedom (typically around 10 kcal/mol at 298 K in the gas phase), while dissociation reactions

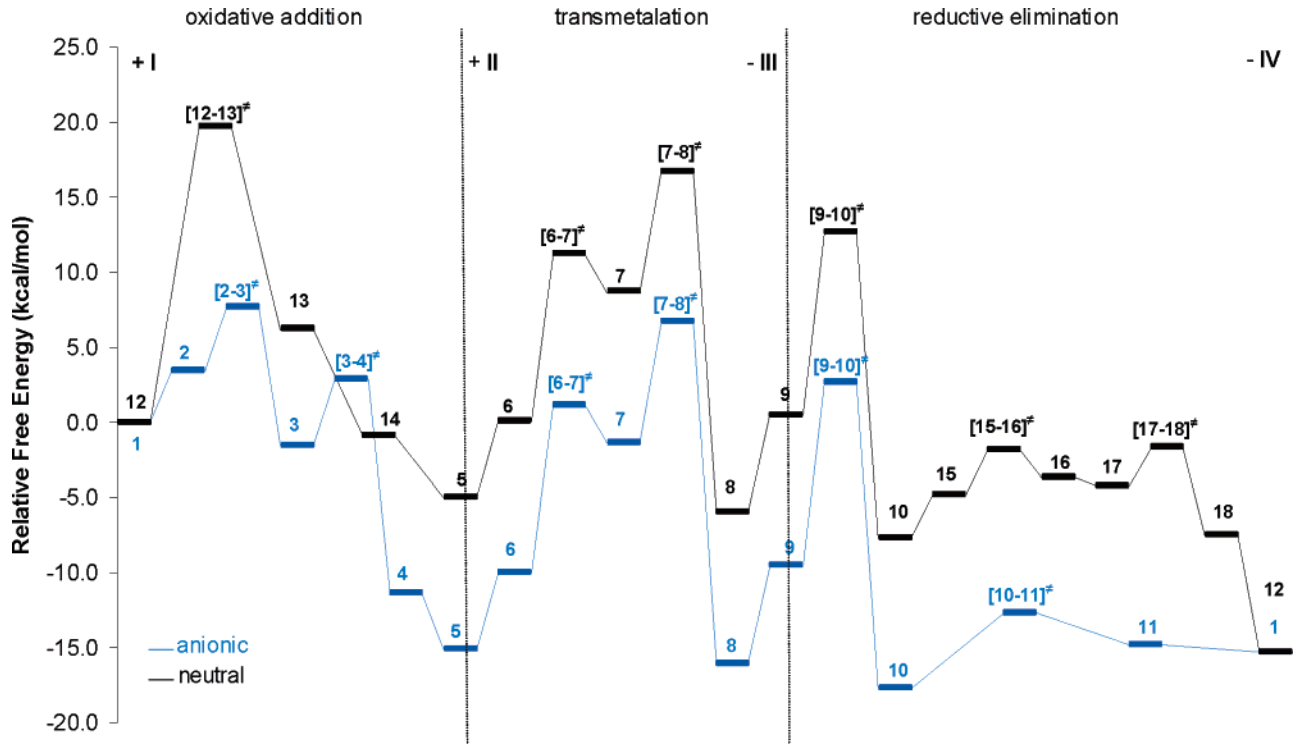

Figure 9. Relative free energies (ΔG_{298} in kcal/mol) for the intermediates and transition states involved in the neutral (black) and anionic (blue) cycle. Conventions see Figure 8.

(liberating products in steps **8** → **9**, **11** → **1**, and **18** → **12**) are entropically favored in an analogous manner. In solution, these entropic effects will be less pronounced than in the gas phase due to solvation and desolvation, but they will still be present to some extent.

The two free-energy profiles in Figure 9 are, of course, again parallel in the central region (**5** → **10**; see above). The final stages of the reductive elimination (beyond **10**) are predicted to be facile on both pathways. The main mechanistic distinction will therefore concern the initial oxidative addition, where the anionic pathway is clearly favored over the neutral pathway, with $\Delta G^{\ddagger}_{298}$ barriers of 7.7 and 19.7 kcal/mol, respectively. This is consistent with the experimental finding that a catalyst generated in situ from palladium(II)acetate is more active than preformed neutral palladium−phosphine complexes since, under these conditions, the formation of three-coordinate anionic complexes is to be expected.[5,6]

Looking at the overall free-energy profiles in Figure 9, it is obvious that there is not a single step that would require excessive activation, and the computed barriers are in a reasonable range for a reaction that occurs experimentally at 60 °C. Within the anionic pathway, the barriers for the initial oxidative addition stage are calculated to be lower than those for later stages, while they are of similar magnitude for the neutral pathway even after accounting for some overestimate for the entropic penalty in **[12−13]**‡. When replacing the PMe_3 ligand by bulkier and less electron-rich phosphine ligands as commonly used in experimental work, the barriers for oxidative addition are generally expected to increase, while those for reductive elimination should decrease. Extrapolating from our current results on the basis of this qualitative expectation, the initial oxidative addition should become mechanistically more important, implying a more pronounced overall preference for the anionic pathway with such ligands.

In conclusion, valuable insights on the mechanism of Pd-catalyzed cross-coupling reactions have been obtained by calculations that provide complete catalytic cycles for a suitable model system. In view of the extreme complexity of the experimentally employed catalytic systems, further studies, especially on triarylphosphine−palladium catalysts, are needed for a more complete understanding of this important transformation.

Acknowledgment. We thank Prof. Dr. A. Jutand for helpful suggestions and discussions. We are grateful to the DFG and the BMBF for financial support. L.J.G. thanks Prof. Dr. M. T. Reetz for his constant encouragement and generous support. D.K. thanks Prof. Dr. V. R. Jensen, Dr. M. Bühl, Dr. H. M. Senn, Dr. S. Vyboishchikov, and H. U. Wüstefeld for fruitful and stimulating discussion.

Supporting Information Available: Energies, graphical representations, geometrical parameters, NPA charges, and Cartesian coordinates of all DFT-optimized structures; complete ref 15. This material is available free of charge via the Internet at http://pubs.acs.org.

JA052435Y